Journal of Interfaces, Thin films, and Low dimensional systems 7 (1) Summer and Autumn (2023) 707-719

The influence of single carbon atom impurity on the electronic transport of two side-closed (6, 0) single-walled boron nitride nanotubes

Scientific research paper

Ali Mohammad Yadollahi[1,2]

[1]*Department of Physics, Ayatollah Amoli Branch, Islamic Azad University, Amol, Iran*

[2]*Department of Physics, Takestan Branch, Islamic Azad University, Takestan, Iran*

ARTICLE INFO

Article history:
Received 2 December 2023
Revised 2 February 2024
Accepted 12 March 2024
Available online 18 March 2024

Keywords
Transmission,
Electronic transport
Boron nitride nanotubes
Negative differential resistance

ABSTRACT

This study utilized Slater-Koster and ForceField methods, along with tight-binding approximation and the NEGF approach, to investigate the impact of a single-carbon atom impurity on the electronic properties of two side-closed (6, 0) single-walled boron nitride nanotubes ((6, 0) TSC-SWBNNTs) positioned at the left, right, and center of the NT. The band gap was notably influenced and reduced due to the introduction of a single-carbon atom impurity. The most significant alterations in the band gap were observed with the presence of the carbon atom impurity at the center of the NT. The comparative analysis of transmission spectrum figures and the density of state figures revealed that at energy points where resonance occurs between the colliding electron and the molecular levels, the transmission coefficient peaks draw near to the molecular levels. This triggers electron transmission and conduction. Despite the regular arrangement of nitrogen and boron atoms on both sides of the NT and the positive interference effect, increasing the bias voltage, particularly at low levels, did not visibly decrease the current. Overall, the presence of negative resistance in the current figure in terms of bias voltage can be utilized as a high-speed electronic switch.

1 Introduction

Recently, nanomaterials have garnered significant attention due to their controllable chemical and physical features and enhanced performance compared to their bulk structures. Carbon nanostructures are extensively investigated for use in various applications from electronics to biomedicine due to their exceptional chemical and physical characteristics. However, boron nitride (BN) nanostructures have attracted even more attention than carbon nanostructures due to their greater thermal and chemical stability and structural similarity with carbon nanomaterials. Among these, one-dimensional BN nanostructures are emerging as novel materials to fulfill some of the needs of various application fields based on their unique and excellent features (i.e., controllable surface, band gap, optical, electronic, thermal, mechanical, and chemical properties). Recently, BN nanomaterials have garnered much attention as the main component; they include nitrogen and boron atom covalent bonds with various crystal lattice structures like cubic BN (c-BN), wurtzite BN, and hexagonal BN (h-BN). BN nanotubes (BNNTs) are structurally similar to carbon NTs (CNTs) because the C atoms in a hexagonal plane are replaced completely by N and B atoms alternately, and there is almost no change in the atomic distance [1].

*Corresponding author.
Email address: a11335533@gmail.com
DOI: 10.22051/jitl.2024.45631.1101

BNNTs were theoretically evaluated in 1994. A year later, they were produced via electric arc discharge. Owing to their cylindrical shape with micrometer length and sub-micrometer diameter, BNNTs have a structure that is highly similar to that of CNTs. However, there are differences between CNTs and BNNTs as the existence of a large band gap of BNNTs provides insulating properties and higher thermal and chemical stability than CNTs [2]. Therefore, they can be used in a wide range of commercial applications due to their unique chemical and physical properties. NTs exist as one or two open and closed ends. Hemispherical caps, at the ends of closed NTs, consisting of hexagons and pentagons, are similar to the structure of fullerene half-molecules [3]. Since their production, CNTs have become the focus of research in various fields due to their unusual tubular structures and exceptional properties. Nonetheless, the higher thermal conductivity, radiation shielding, nontoxicity, and insulating properties of BNNTs are superior to those of CNTs, facilitating the use of BNNTs in several fields, such as aerospace engineering and different biomedical applications, particularly in the transfer of anticancer drugs and tissue engineering [1]. Studies on magnetic features [4], tunability of electronic characteristics [5] of BNNTs, and molecular dynamics studies [6], such as tight-binding technique, density functional theory, as well as valence layer model in BNNTs, suggest that BNNTs can be employed as a supernumerary for CNTs [7].

The key difference between BNNTs and CNTs is the ionic bond between boron and nitrogen atoms, changing the molecular orbital configuration [8]. These differences cause changes in molecular electronics, optical properties, and solid-state [9]. For instance, BNNTs present good electrical insulation owing to their band gaps [11, 10], namely, a band gap energy difference between 5 and 6 eV, enabling BNNTs to release ultraviolet light when excited by electrons or phonons [9].

Isaki [12] was the first to report the occurrence of negative differential resistance in pn junction with high impurity density. These devices have garnered significant attention from researchers due to their wide range of applications in circuits such as solar cells and microwave amplifiers. To observe negative differential resistance, Isaki's tunnel current must drop to zero within the voltage range of 0.3V to 0.6V [13, 14]. In this device, when unbiased, the capacitance band of the p region is positioned higher than the conduction band level of the n region at the interface. As the voltage increases in direct bias, the capacitance band level of the p-type region decreases and aligns with the conduction band level of the n-type region. This process reduces the difference in energy levels between holes in the p region and electrons in the n region, allowing electrons to tunnel from the conduction band of the n region to the capacitance band of the p region, known as band-to-band tunneling current. As the voltage gradually increases, the capacitance band of the p region moves closer to the surface of the conduction band of the n region, leading to an increase in their overlap and subsequently increasing the tunneling current. This rise continues until the bands are aligned, resulting in the peak current. Subsequently, as the voltage increases further, the distance between the bands increases, causing a decrease in tunnel current, known as negative differential resistance. This decrease persists until the voltage reaches the diode's threshold voltage, with the lowest current point referred to as the valley current. Beyond the threshold voltage, the device current rises exponentially with the voltage, resembling a conventional diode [15].

Although nanomaterials without defects have attractive physical features, in reality, defects are inevitable, and BNNTs are usually not without defects experimentally [16-20]. Such defects include impurities, vacancies, and Stone-Wales defects, considerably affecting the properties of BNNTs [16, 17]. Research indicates that by substituting a carbon element rather than boron or nitrogen in the BNNT, the NT can be converted into a p-type or n-type semiconductor, as by replacing a carbon atom with boron, an electron is added, while a hole is created by substitution of a carbon atom with nitrogen [21, 22]. This work evaluated the electronic properties of two side-closed (6, 0) single-walled boron nitride NTs ((6, 0) TSC-SWBNNTs) in its pure state and with the impurity of one carbon atom in place of nitrogen and boron atoms in the center, left, and right sides of these NTs. The transmission spectrum, Density of States (DOS), and bias current-voltage figures are drawn for each of the states. Additionally, the presence of negative differential resistance has been investigated for the above-mentioned states.

2 Simulation method

Considering the vast number of atoms involved, the valid ATK simulator software has been utilized in this study. QuantumATK offers access to a powerful collection of simulation tools to analyze various types of systems, including density functional theory, classical potentials, semi-experimental tight-binding, and non-equilibrium Green's functions (NEGF) [23, 24]. The foundation of this software is Python, which is a robust and high-level programming language. Slater-Koster [21] and ForceField [25] methods, as well as tight-binding approximation and NEGF approach, have been employed in this software. Both ends of the NT have been capped using hexagons and pentagons composed of nitrogen and boron atoms. The axis of the (6, 0) TSC-SWBNNTs is considered parallel to the z-axis. The Mesh cut-off is set to 150 Rydberg during the simulation [26, 27]. The Brillouin zone is characterized by a K-point of 1×1×100 [28-32]. Additionally, a force tolerance of 0.01 eV/Å with a maximum step of 500 has been applied to optimize the device. CNT (5, 5) with a repetition number of 1×1×4 has been utilized in the electrodes. The (6, 0) TSC-SWBNNT, before being positioned between two electrodes, was optimized to ensure its atoms were in the lowest energy state. This process of optimization was carried out for both its pure state as well as when it contained impurities in the form of carbon atoms. The (6, 0) TSC-SWBNNT was then inserted between two electrodes on the left and right, which were constructed from CNT (5, 5). Notably, there was no bond between the electrodes and the central region, resulting in electron transport occurring solely through tunneling. This mechanism is reminiscent of a diode, with the left and right electrodes functioning as the source and drain respectively. Upon applying different bias voltages across the left and right electrodes, data pertaining to transmission, density of states (DOS), and current as a function of voltage were gathered. This data was then graphically represented using MATLAB software. The aforementioned procedure were carried out for both the pure and carbon atom impurity states of the central, left and right (6, 0) TSC-SWBNNT. Program implementation was started after making the (6, 0) TSC-SWBNNTs and optimizing and making the aforementioned settings.

Based on NEGF relationships, the transmission function T (E, V) with energy E and bias voltage V is [33, 34]:

$$T(E,V) = Tr[\Gamma_L(V)G^R(E,V)\Gamma_R(V)G^A(E,V)], \quad (1)$$

Where G^A and G^R are the advanced and retarded Green's functions of the central scattering area, respectively. Further, $\Gamma_{LR} = i[\sum^R_{L(R)}(E) - \sum^A_{L(R)}(E)]$ shows the broadening function. Ultimately, $\sum^R_{L(R)}(E)$ and $\sum^A_{L(R)}(E)$ represent the self-energies of the central scattering area including all the impacts of the electrodes [33, 34].

System current is stated using the Land Landauer-Butikker equation [35-37]:

$$I(V) = \frac{2e}{h}\int [f(E-\mu_L) - f(E-\mu_R)]T(E,V)dE, \quad (2)$$

where e, h, and $f(E-\mu_{L(R)})$ denote the electron electrical charge, Planck's constant, and the Fermi distribution function of the electrons on the left (right) side, respectively, and $\mu_{L(R)}$ shows the left (right) electrode's electrochemical potential [35-37].

3 Results and discussion

As depicted in Figure 1, the total number of nitrogen and boron atoms in the (6, 0) TSC-SWBNNT equals 112 atoms. Additionally, the diameter of the (6, 0) TSC-SWBNNT and its length measure approximately 5.8 and 19.9 angstroms, respectively (Figure 2). The two sides of the (6, 0) TSC-SWBNNT have been closed with nitrogen and boron atoms in the form of hexagonal and pentagonal structures. The axis of the (6, 0) TSC-SWBNNT is parallel to the z-axis.

According to Figures 3a to 3g, a single carbon atom is substituted with nitrogen and boron atoms in the central sections (Figures 3a and 3b), left (Figures 3c and 3d), and right (Figures 3e and 3f). Replacing a boron atom with a carbon atom introduces an extra electron into the Lumo level of the (6, 0) TSC-SWBNNTs due to carbon's additional electron. This impurity changes the (6, 0) TSC-SWBNNT into an n-type semiconductor. Replacing a nitrogen atom with a carbon atom introduces a hole into the homo level of the (6, 0) TSC-SWBNNT due to carbon's fewer electrons. This

impurity transforms the (6, 0) TSC-SWBNNT into a p-type semiconductor. [37, 39, 31]. According to the periodic table, carbon is more electronegative than boron, and nitrogen is more electronegative than carbon. Therefore, by substituting the carbon atom with either nitrogen or boron atoms, the bond length between the substituted carbon atom and the surrounding atoms changes upon device optimization. Consequently, the bond length in the presence of a carbon atom is also affected and altered. Hence, both factors of introducing an additional electron or hole and changing the bond length need to be considered together. Moreover, according to Eq. (1), the transmission coefficient depends on two factors: the electronic energy of the molecule and the strength of the electrode/molecule coupling. Therefore, altering the bond length and converting the NT to n-type or p-type can both influence the transmission coefficient.

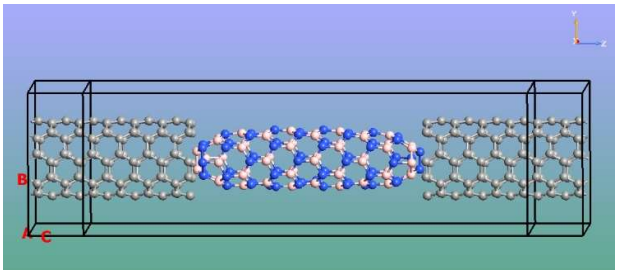

Figure 1. The tool made with pure (6, 0) TSC-SWBNNTs and 2 carbon nanotube electrodes (5, 5) on both sides.

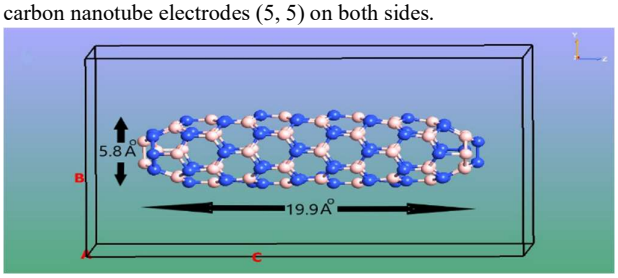

Figure 2. (6, 0) TSC-SWBNNT.

A bias voltage ranging from 0 to 5 V has been applied between the two right and left electrodes. For the energy range of -5 to 5 eV and with an accuracy of 0.1 eV, the transmission spectrum has been depicted in Figures 4a to 4f for three bias voltage values of 0, 2.5, and 5 V. Since electrons with Fermi energy play the most significant role in the electronic transport process, transmission coefficients have been illustrated around the Fermi level. Four figures have been presented for each configuration, including one state without impurity and three states with the impurity of one carbon atom in the left, right, and center of the (6, 0) TSC-SWBNNTs. The transmission figure changes for different states considering the presence of a carbon atom impurity in this structure.

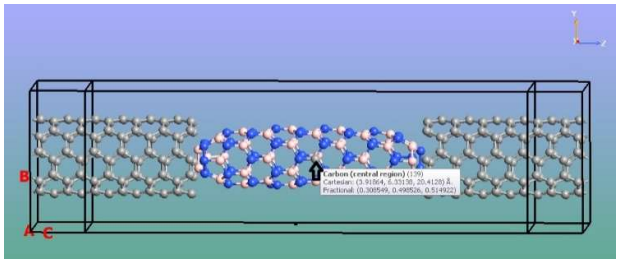

Figure 3a. The tool created with (6, 0) TSC-SWBNNT with carbon atom impurity rather than boron atom in the center and two (5, 5) carbon nanotube electrodes on the two sides.

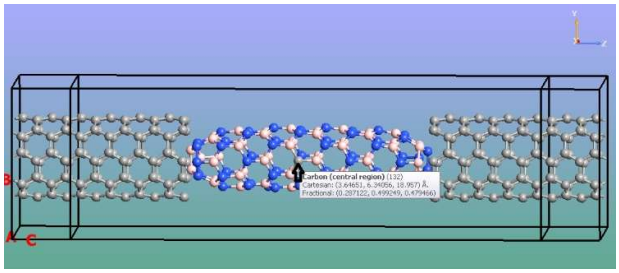

Figure 3b. The tool generated with (6, 0) TSC-SWBNNT with carbon atom impurity in place of two (5, 5) carbon nanotube electrodes on the two sides and nitrogen atom in the center.

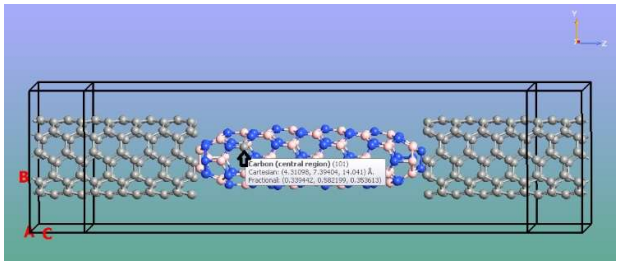

Figure 3c. The tool created with (6, 0) TSC-SWBNNT with carbon atom impurity rather than two (5, 5) carbon nanotube electrodes on the two sides and boron atom on the left side.

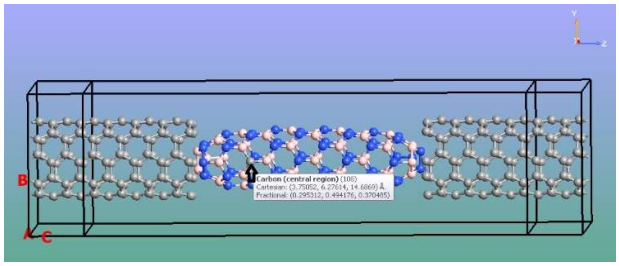

Figure 3d. The tool generated with (6, 0) TSC-SWBNNT with carbon atom impurity rather than two (5, 5) carbon nanotube electrodes on the two sides and nitrogen atom on the left side.

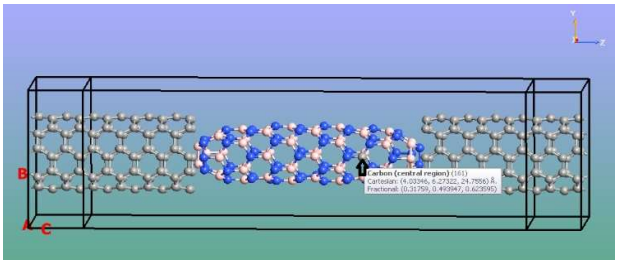

Figure 3e: The tool made with (6, 0) TSC-SWBNNT with carbon atom impurity rather than two (5, 5) carbon nanotube electrodes on the two sides and boron atom on the right side.

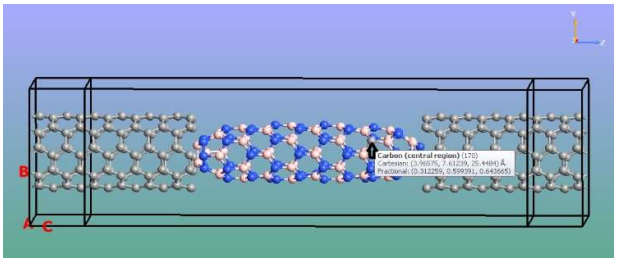

Figure 3f. The tool created made with (6, 0) TSC-SWBNNT with carbon atom impurity rather than two (5, 5) carbon nanotube electrodes on the two sides and nitrogen atom on the right side.

In Figure 4a, peaks on the left and right sides of the figure for the pure state begin at -2.4 V and +1.1 V, respectively. The band gap from the left side is significantly reduced by substituting the carbon atom with nitrogen according to the figures [40]. This reduction occurs because when carbon is replaced with nitrogen, the (6, 0) TSC-SWBNNTs undergo electron reduction and transform into a p-type semiconductor. Additionally, the number of holes increases in the valence band, leading to a decrease in the band gap from the left side of the figure. Furthermore, the most significant band gap changes in this scenario are associated with the carbon atom impurity rather than nitrogen in the center. The presence of a high number of holes and electrons near the electrodes and on both sides of the NT, coupled with irregularities in those areas, minimizes the impact of impurities. However, the replacement of a carbon atom with nitrogen has a more noticeable effect at the center of the NT due to greater regularity in that region. When carbon impurity is substituted for boron, the band gap slightly decreases from the right side of the figure. When carbon substitutes for boron in (6, 0) TSC-SWBNNTs, they transition into n-type semiconductors due to an increase in electrons. Consequently, the number of electrons in the conduction band rises, leading to a reduction in the band gap, as indicated on the right side of the figure. Further, most changes in the band gap in this case are associated with carbon atom impurity rather than the boron in the center. Due to the abundance of holes and electrons near the electrodes and on both sides of the NT, along with less regularity in those regions, the impurity's effect is negligible. However, the effect of the replacement of the carbon atom in place of boron is more evident in the center of the NT because of the presence of more regularity. Certainly, the replacement of carbon with nitrogen and boron leads to changes in bond lengths across various states under consideration. As a result, the shape of transmission spectrum figures is altered on both the left and right sides. The height of the peaks decreases with increasing bias voltage. Furthermore, the sharpness of the curves' peaks in Figures 4c and 4d increases as the bias voltage is incremented to 2.5 V, while their width slightly decreases, indicating greater localization of conduction electrons. This trend of increasing peak sharpness at a bias voltage of 5 V is illustrated in Figures 4e and 4f. Furthermore, it is notable that the peaks on the right side of the curves exhibit greater height compared to those on the left side. This discrepancy underscores the stronger influence of electrons at positive energies relative to the impact of holes at negative energies. Similarly, as the bias voltage increases, the height of the peaks decreases, indicating increased localization of holes and electrons.

Figures 5a and 5b display the density of states (DOS) for the (6, 0) TSC-SWBNNT in its pure state and with the impurity of one carbon atom, instead of nitrogen and boron atoms, at the center, as well as the right and left sides of the NT. The DOS of a system describes the number of states available for occupation in each energy interval at each energy level [41]. Upon comparing the DOS figures with transmission spectrum figures, it becomes evident that transmission coefficient peaks closely align with molecular levels. This alignment signifies electron transmission and conduction, occurring at energy points where resonance takes place between collision electrons and molecular levels. Equation (1) demonstrates that the transmission coefficient is determined by the electronic energy of the molecule and the strength of the electrode/molecule coupling. Therefore, the Green's function and subsequently the density of states (DOS) of the coupled molecule, as well as the transmission spectrum, change with variations in the electronic energy of the coupled molecule. Consequently, large values of the

transmission spectrum are observed close to the molecular levels of the (6, 0) TSC-SWBNNT.

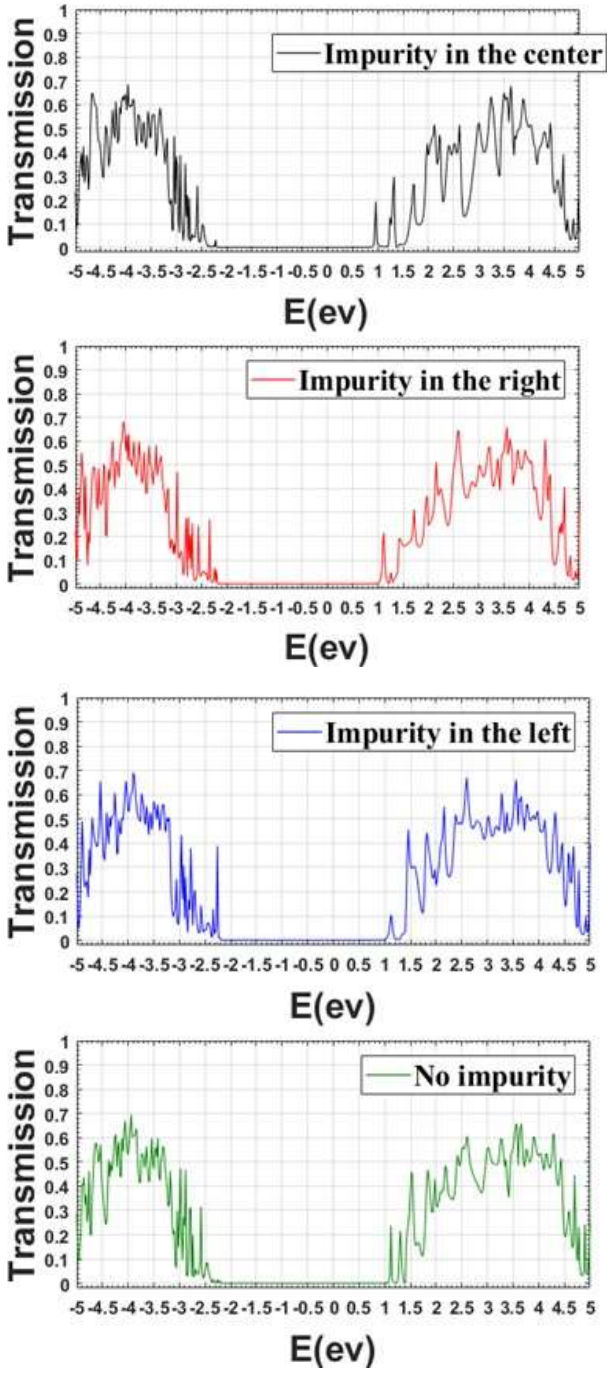

Figure 4a. The transmission spectrum figure for a (6, 0) TSC-SWBNNTs at zero bias voltage in the pure state and impurity of one carbon atom in place of one boron atom in the three sections of the left, right and central nanotube.

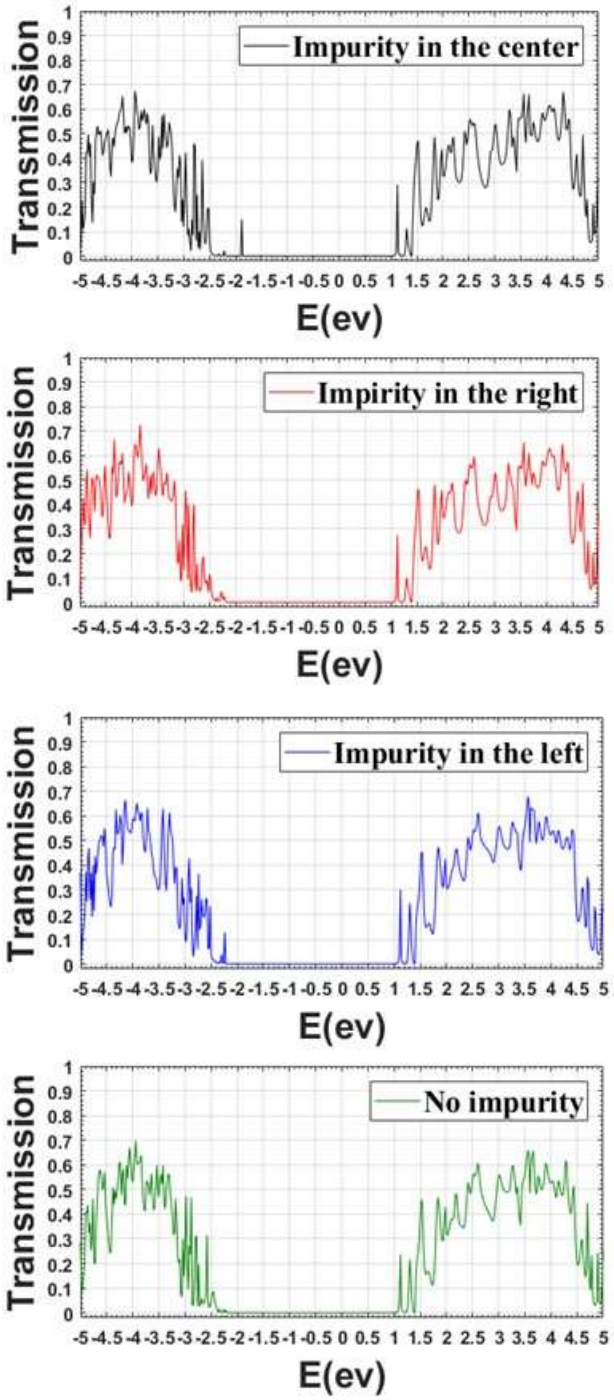

Figure 4b. Transmission spectrum figure for (6, 0) TSC-SWBNNTs at zero bias voltage in the pure state and impurity of a carbon atom in place of a nitrogen atom in the three sections of the left, right and central nanotube.

In conventional transport, it is assumed that the electron wave function spreads uniformly throughout the system. Thus, when the energy of the electron is approximately equal to the molecular level, significant transmission occurs, allowing the electron to pass through the molecule resonantly.

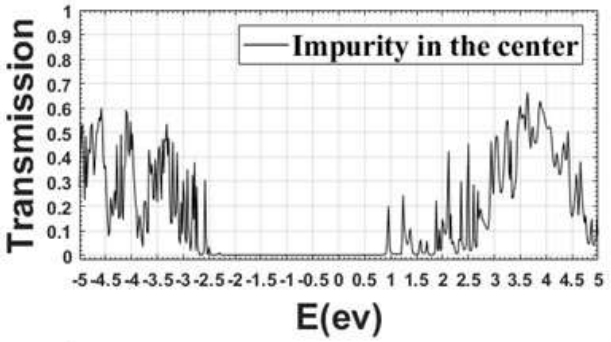

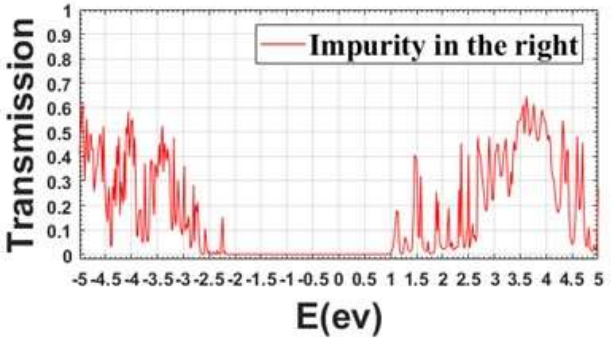

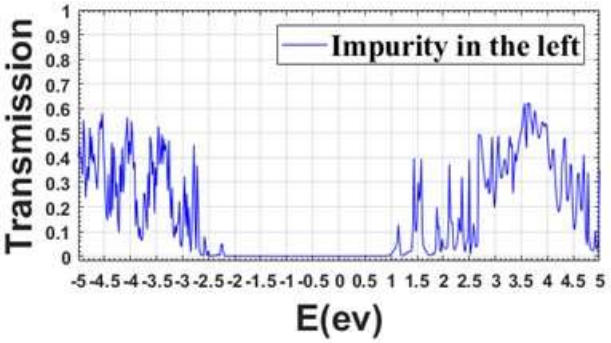

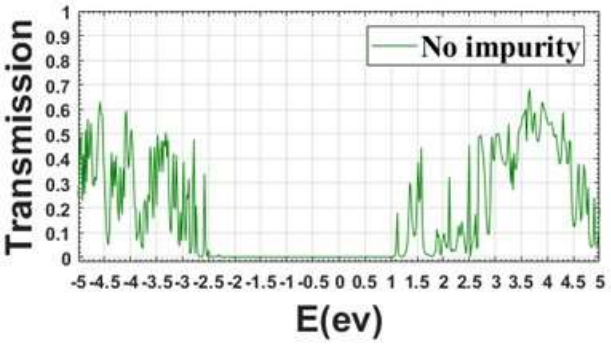

Figure 4c. Transmission spectrum figure for a (6, 0) TSC-SWBNNTs at a bias voltage of 2.5 V in the pure state and impurity of a carbon atom in place of a boron atom in the three sections of the right, left, and central nanotube.

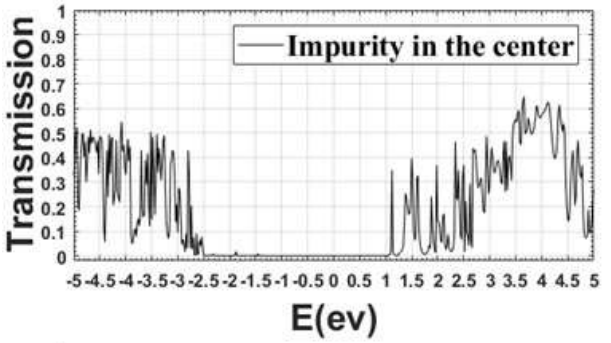

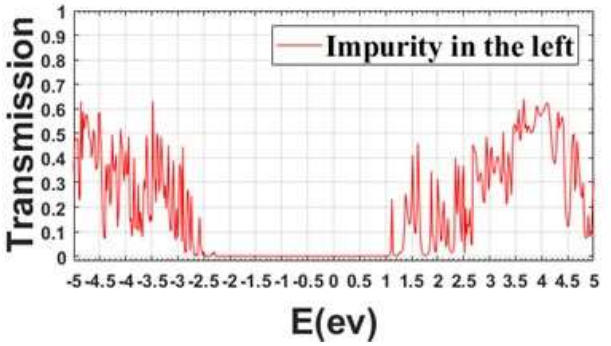

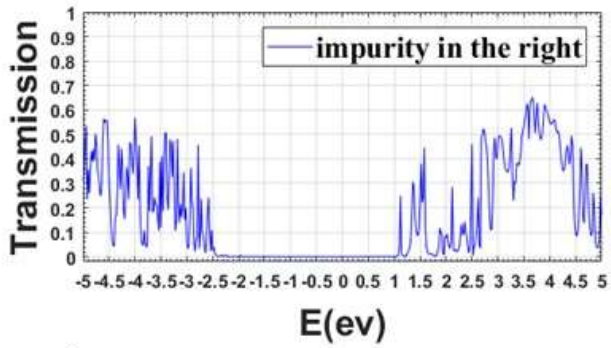

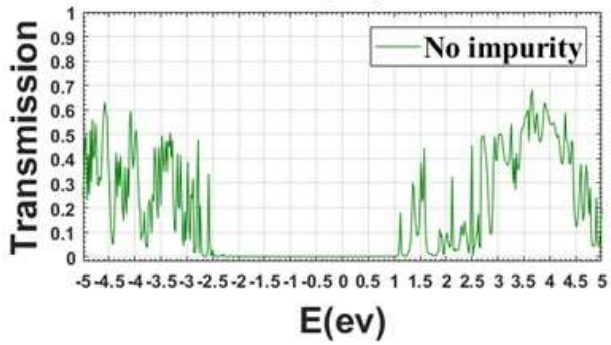

Figure 4d. The transmission spectrum figure for a (6, 0) TSC-SWBNNTs at a bias voltage of 2.5 V in the pure state and impurity of a carbon atom in place of a nitrogen atom in the 3 sections of the left, right, and central nanotube.

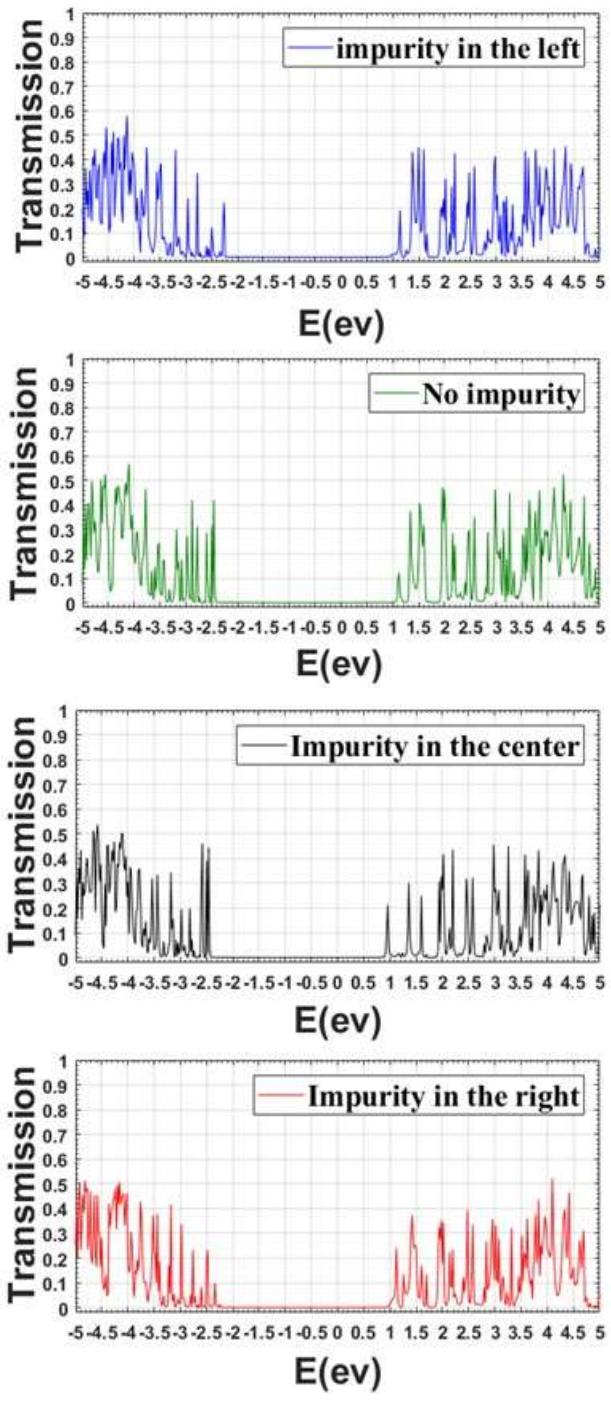

Figure 4e. The transmission spectrum figure for a (6, 0) TSC-SWBNNTs at a bias voltage of 5 V in the pure state and impurity of a carbon atom in place of a boron atom in the three sections of the left, right and central nanotube.

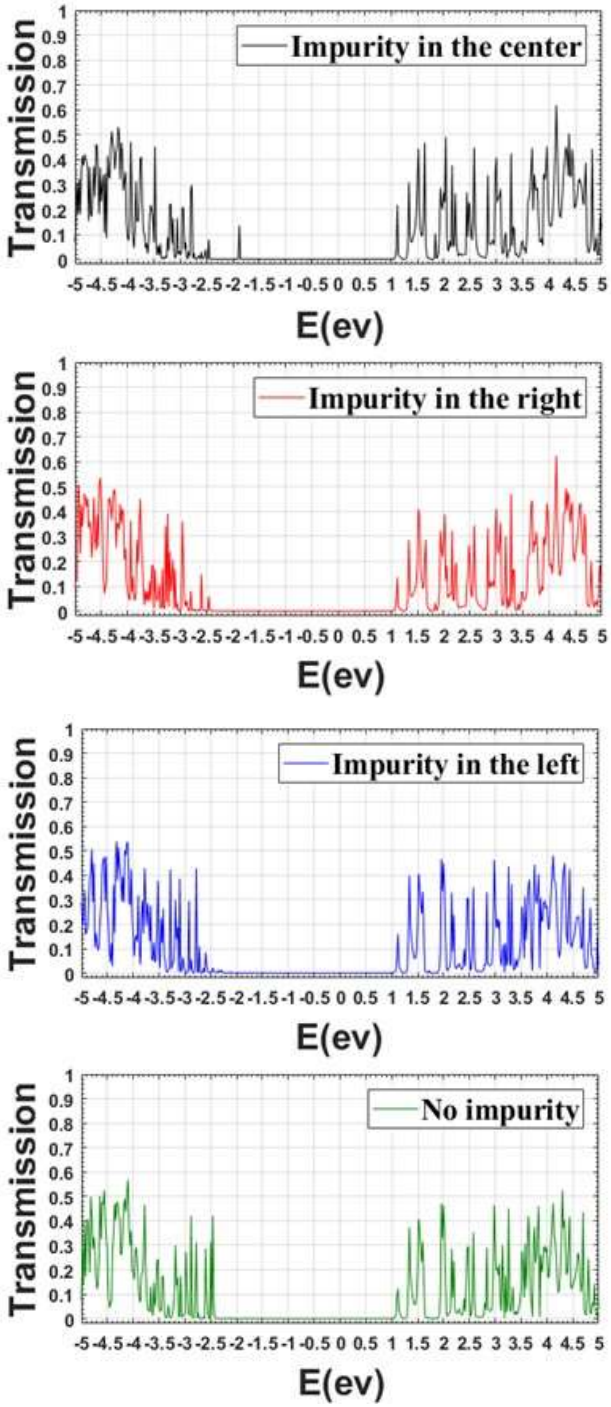

Figure 4f. transmission spectrum figure for (6, 0) TSC-SWBNNTs at a bias voltage of 5 V in the pure state and impurity of a carbon atom in place of a nitrogen atom in the three sections of the left, right and central nanotube.

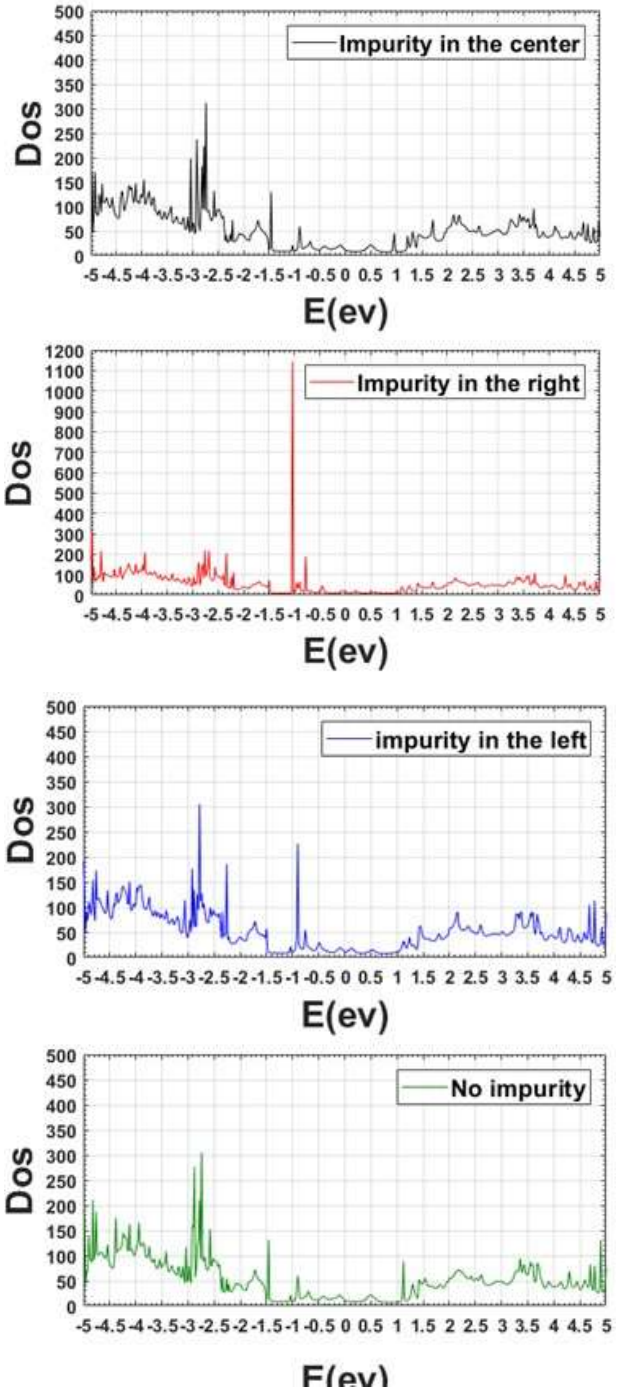

Figure 5a. DOS figure for (6, 0) TSC-SWBNNTs in pure state and impurity of one carbon atom in place of boron atom in the 3 sections of the left, right and center of the nanotube.

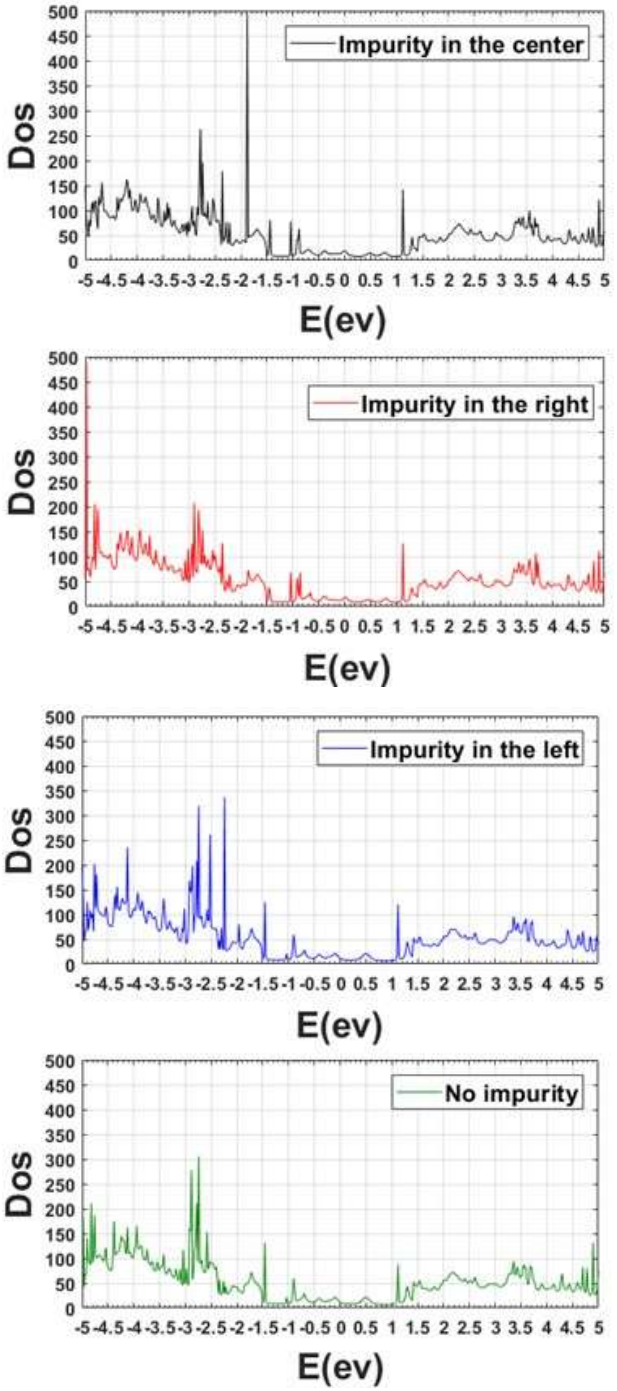

Figure 5b. Dos figure for (6, 0) TSC-SWBNNTs in pure state and impurity of one carbon atom instead of nitrogen atom in the 3 sections of the left, right and center of the nanotube.

Figures 6a and 6b depict the current characteristics as a function of the bias voltage. A bias voltage ranging from 0 to 5 V has been applied between the left and right electrodes. A threshold voltage is necessary to initiate current flow through the device, indicating that the device is in the off state at low applied voltages. Consequently, there is no peak near the Fermi energy. The staircase behavior of the I-V curves can be explained by the transmission coefficient curve (Figures 4a to 4f). Assuming $E_F = 0$, the interval of the bias or the integral interval in the total current integral is actually $[-V_b/2, V_b/2]$. Additionally, the total current is equal to the area under the transmission spectrum curve in the bias interval [Eq. (2)]. Clearly, the current significantly increases when a new peak, induced by increasing the bias voltage, enters the bias interval (opening a new channel). As the bias voltage increases, the current curves exhibit an increase in a staircase manner. At the points where the staircase behavior occurs, there is a sudden jump in the current increase, indicating the occurrence of new tunneling events. The replacement of a carbon atom with a boron atom results in the creation of an additional electron, transforming the material into an n-type semiconductor, thereby increasing electron presence at the carbon atom's location and reducing current. Conversely, electron absorption due to carbon atom replacement by nitrogen creates an extra hole in (6, 0) TSC-SWBNNTs, forming a p-type semiconductor and leading to a slight increase in current. Despite the regular arrangement of boron and nitrogen atoms at both ends of the NT and the positive interference effect observed, no significant decrease in current is observed with increasing bias voltage in the current figures relative to the bias voltage. Likewise, negative resistance can be observed at a high bias voltage in Figures 6a and 6b.

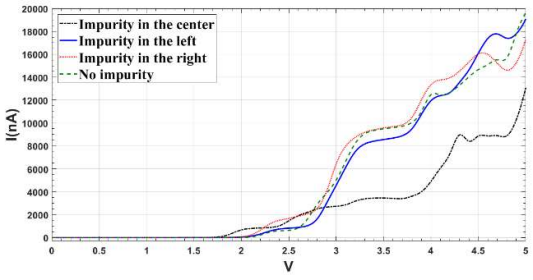

Figure 6a. Current-voltage figure for (6, 0) TSC-SWBNNTs pure and impurity state of a carbon atom in place of boron atom in the three sections of the left, right and center of the nanotube.

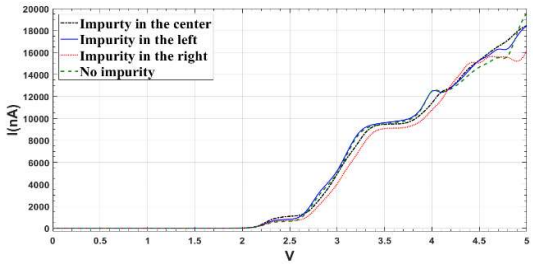

Figure 6b. Current-voltage figure for (6, 0) TSC-SWBNNTs pure state and impurity of a carbon atom in place of nitrogen atom in the 3 sections of the left, right and center of the nanotube.

Figures 7a and 7b depict the current differential/voltage differential ratio for bias voltages ranging from 0 to 5 V. Additionally, Figures 7a and 7b illustrate the system's conduction as changes in differential (dI/dV). Comparing Figures 7a and 7b, it is evident that the height of the peaks in Figure 7a is larger than that in Figure 7b; in other words, the conduction is stronger in the case where carbon is substituted instead of boron. Furthermore, Figures 7a and 7b demonstrate that the differential conduction can have both negative and positive values. They also indicate the negative slope of the curve, signifying negative resistance.

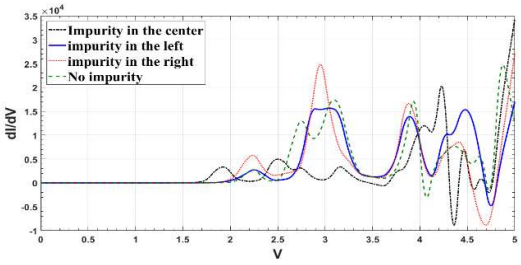

Figure 7a. dI/dV figure in terms of voltage for (6, 0) TSC-SWBNNT pure and impurity state of a carbon atom instead of boron atom in the three sections of the left, right and center of the nanotube.

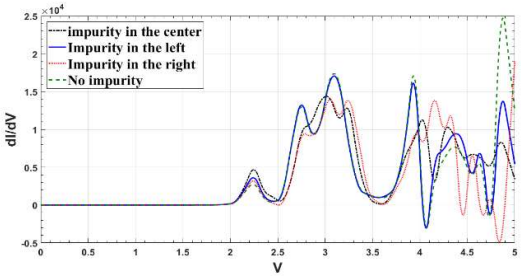

Figure 7b. dI/dV figure in terms of voltage for (6, 0) TSC-SWBNNT pure and impurity state of a carbon atom in place of nitrogen atom in the three sections of the left, right and center of the nanotube.

Comparing the findings of this study with experimental data shows that impurities play an important role in changing the band structure and density of states of boron nitride nanotubes. Experimental research show that the presence of impurities changes the band gap [10, 11].

4 Conclusions

This study, with using Slater-Koster and ForceField methods, as well as tight-binding approximation and NEGF approach, investigated the effect of impurity of single-carbon atom on the electronic properties of two side-closed (6, 0) single-walled boron nitride nanotubes ((6, 0) TSC-SWBNNTs) in the left, right, and center of the NT. The current study evaluated the effect of single-carbon atom impurity on the electronic properties of a (6, 0) TSC-SWBNNT at the right, left, and center positions within the NT. The presence of a single-carbon atom impurity could influence the band gap, slightly reducing it. The most significant change in the band gap was observed with the impurity of the carbon atom at the center position. In comparing the transmission spectrum figures with the DOS figures, it is observed that at energy points where resonance occurs between the collision electrons and molecular levels, the peaks of the transmission coefficient align closely with the molecular levels. This alignment facilitates electron transfer, results in conduction. In this case, an increase in the current figure with respect to the bias voltage could be observed in a staircase pattern. Additionally, despite the regular arrangement of nitrogen and boron atoms at the two ends of the NT and the positive effect of the interference phenomenon at these ends, no significant decrease in the current magnitude was observed with increasing the bias voltage in the current figures. Consequently, negative resistance could be detected at high bias voltage.

References

[1] E. A. Turhan et al. “Properties and applications of boron nitride nanotubes”. Nanotechnology, **33** (2022) 242001. DOI: https://doi.org/10.1088/1361-6528/ac5839.

[2] X. Blasé et al. “Stability and Band Gap Constancy of Boron Nitride Nanotubes”. EuroPhysics. Letters, **28** (1994) 335-340. DOI: 10.1209/0295-5075/28/5/007.

[3] R. Cruz-Silva et al. “Fullerene and nanotube growth: new insights using first principles and molecular dynamics”. Philosophical Transactions of the Royal Society A, **374** (2016) 20150327. DOI: https://doi.org/10.1098/rsta.2015.0327.

[4] R. Wu et al. “Magnetism in BN nanotubes induced by carbon doping”. Applied Physics Letters, **86** (2005) 122510. DOI: https://doi.org/10.1063/1.1890477.

[5] K. Khoo et al. “Tuning the electronic properties of boron nitride nanotubes with transverse electric fields: A giant dc Stark effect”. Physical Review B, **69** (2004) 201401. DOI: https://doi.org/10.1103/PhysRevB.69.201401.

[6] C. Y. Won et al. “Structure and Dynamics of Water Confined in a Boron Nitride Nanotube”. The Journal of Physical Chemistry C, **112** (2008) 1812–8. DOI: https://doi.org/10.1021/jp076747u.

[7] T. Schmidt et al. “Theoretical study of native defects in BN nanotubes”. Physical Review B, **67** (2003) 113407. DOI: 10.1103/PhysRevB.67.113407.

[8] Z. Liu et al. “B-N versus C-C: How Similar Are They?”. Angewandte Chemie International Edition, **47** (2008) 242–4. DOI: 10.1002/anie.200703535.

[9] S. Dolati et al. “A Comparison Study between Boron nitride Nanotubes and Carbon Nanotubes”. International Journal of Emerging Technology and Advanced Engineering, **2** (2012) 470-474.

[10] M. Terrones Maldonado et al. “Pure and doped boron nitride nanotubes”. Materials Today, **10** (2007) 30–8. DOI: https://doi.org/10.1016/S1369-7021(07)70077-9.

[11] D. Golberg et al. “Boron Nitride Nanotubes”. Advanced. Materials, **19** (2007) 2413–32. DOI: https://doi.org/10.1002/adma.200700179.

[12] L. Esaki "New phenomenon in narrow germanium p− n junctions." Physical review, **109** (1958) 603. DOI: https://doi.org/10.1103/PhysRev.109.603.

[13] M. Oehme et al. "Very High Room-temperature peak-to-valley current ratio in Si Esaki tunneling diodes (March 2010)." IEEE transactions on electron devices, **57**(2010) 2857-2863. DOI: 10.1109/TED.2010.2068395.

[14] W. Y. Fung et al. "Esaki tunnel diodes based on vertical Si-Ge nanowire heterojunctions." Applied Physics Letters, **99** (2011) 092108. DOI: https://doi.org/10.1063/1.3633347.

[15] S. M. Sze et al. "Physics of Semiconductor Devices." (2006) A. P. - 832 pages.

[16] E. Almahmoud et al. "Band gap tuning in carbon doped boron nitride mono sheet with Stone Wales defect: a simulation study". Materials Research Express, **6** (2019) 105038. DOI: https://doi.org/10.1088/2053-1591/ab39a3.

[17] I. Petrushenko et al. "Stone-Wales Defects in Graphene-like Boron Nitride-Carbon Heterostructures: Formation Energies, Structural Properties, and Reactivity". Computational Materials Science, **128** (2017) 243-248. DOI: https://doi.org/10.1016/j.commatsci.2016.11.039.

[18] J. F. Jia et al. "The structure and electronic property of BN nanotube". Physica B Condensed Matter, **381** (2006) 90-95. DOI: https://doi.org/10.1016/j.physb.2005.12.258.

[19] J. X. Zhao et al. "A theoretical study on the conductivity of carbon doped BNNT". Journal of the Chinese Chemical Society, **52** (2005) 395-398. DOI: https://doi.org/10.1002/jccs.200500059.

[20] A. Talla Jamal et al. "Structural characterization of deformed boron nitride nanotubes". Journal of Computational and Theoretical Nanoscience, **11** (2014) 1838-1843. DOI: https://doi.org/10.1166/jctn.2014.3576.

[21] D. A. Papaconstantopoulos et al. "The Slater–Koster tight-binding method: a computationally efficient and accurate approach". Journal of Physics: Condensed Matter, **15** (2003) 413–440. DOI: 10.1088/0953-8984/15/10/201.

[22] L. Ci. "Atomic layers of hybridized boron nitride and graphene domains". Nature Materials, **9** (2010) 430–435. DOI: https://doi.org/10.1038/nmat2711.

[23] A. Pecchia et al. "Non-equilibrium Green's functions in density functional tight binding: method and applications". New Journal of Physics, **10** (2008) 065022. DOI: 10.1088/1367-2630/10/6/065022.

[24] M. D. Ganji et al. "Density functional non-equilibrium Green's function (DFT-NEGF) study of the smallest nano-molecular switch". Physica E: Low-dimensional Systems and Nanostructures, **40** (2008) 2606-2613. DOI: https://doi.org/10.1016/j.physe.2007.09.123.

[25] J. Schneider et al. "ATK-ForceField: a new generation molecular dynamics software package". Modelling and Simulation in Materials Science and Engineering, **25** (2017) 085007. DOI: 10.1088/1361-651X/aa8ff0.

[26] P. Zhao et al. "Rectifying behavior in nitrogen-doped zigzag single-walled carbon nanotube junctions". Solid State Communications **152** (2012) 2040–2044. DOI: https://doi.org/10.1016/j.ssc.2012.08.013.

[27] M. Wang et al. "Spin transport properties in Fe-doped graphene/hexagonal boron-nitride nanoribbons heterostructures". Physics Letters A **383** (2019) 2217-2222. DOI: 10.1016/j.physleta. 2019.04.022.

[28] T. Markussen et al. "Surface-Decorated Silicon Nanowires: A Route to High-ZT Thermoelectrics". Physical Review Letters, **103** (2009) 055502(4). DOI: https://doi.org/10.1103/PhysRevLett.103.055502.

[29] A. M. Yadollahi et al. "Thermoelectric properties of two sided-closed single-walled boron nitride nanotubes (6, 3)". Indian Journal of Physics, **96** (2022) 3493–3500. DOI: https://doi.org/10.1007/s12648-021-02255-2.

[30] A. M. Yadollahi et al. "Effect of temperature changes on thermoelectric properties of the two sided-closed single-walled BNNTs (6, 3).

Journal of Interfaces". Thin Films, and Low dimensional systems, **5** (2022) 421-427. DOI: 10.22051/jitl.202.40200.1072.

[31] A. M. Yadollahi et al. "Effect of impurity and temperature changes on the thermoelectric properties of the (6, 3) two sided-closed single-walled boron nitride nanotubes ((6, 3) TSC-SWBNNTs)". Journal of Theoretical and Applied Physics, **16** (2022) 162230-162240. DOI: 10.30495/jtap. 162230.

[32] R. Sadeghi et al. "Thermoelectric properties of zigzag single-walled Carbon nanotubes and zigzag single-walled Boron Nitride nanotubes (9, 0)". International Journal of Nano Dimension, **13** (2022) 311-319. DOI: 10.22034/IJND.2022.1951622.2118.

[33] P. Zhao et al. "Rectifying behavior in nitrogen-doped zigzag single-walled carbon nanotube junctions". Solid State Communications, **152** (2012) 2040–2044. DOI: https://doi.org/10.1016/j.ssc.2012.08.013.

[34] S. Datta. "Electronic Transport in Mesoscopic Systems". Cambridge University Press, New York, (1995).

[35] P. Chaudhuri et al. "Density functional study of glycine adsorption on single-walled BN nanotubes". Applied Surface Sciences, **536** (2020) 147686. DOI: 10.1016/j.apsusc.2020.147686.

[36] J. X. Zhao et al. "A Theoretical Study on the Conductivity of Carbon Doped BNNT". Journal of the Chinese Chemical Society, **52** (2005) 395-398. DOI: https://doi.org/10.1002/jccs.200500059.

[3] C. Rui et al. "Transport properties of B/P doped grapheme nanoribbon field-effect transistor". Materials Science in Semiconductor Processing, **130** (2021) 105826. DOI: https://doi.org/10.1016/j.mssp. 2021. 105826.

[38] L. Song. "Large scale growth and characterization of atomic hexagonal boron nitride layers". Nano Letters, **10** (2010) 3209–3215. https://doi.org/10.1021/nl1022139.

[39] M. R. Roknabadi et al. "Electronic and optical properties of pure and doped boron-nitride nano". Physica. B, **410** (2013) 212–216. DOI: https://doi.org/10.1016/j. physb.2012.10.033.

[40] Ali Mohammad Yadollahi1 et al." The influence of single carbon atom impurity on the electronic transport of (6, 3) two side-closed single-walled boron nitride nanotubes". Journal of Molecular Modeling, **29** (2023) 133. DOI: https://doi.org/10.1007/s00894-023-05493-9.

[41] M. Yaghobi et al. "Electronic transport through a C_{60-n} X_n (X=N and B) molecular bridge". Molecular Physics, **109** (2011) 1821–1829. DOI: 10.1080/00268976.2011.593567.